

Forces in the isotropic phase of a confined nematic liquid crystal 5CB

K. Kočevar

J. Stefan Institute, Jamova 39, 1000 Ljubljana, Slovenia

I. Muševič*

*Faculty of Mathematics and Physics, University of Ljubljana, Jadranska 19, 1000 Ljubljana, Slovenia**and J. Stefan Institute, Jamova 39, 1000 Ljubljana, Slovenia*

(Received 15 May 2001; published 24 October 2001)

Using a temperature controlled atomic force microscope, we have measured the temperature dependence of the force between a flat silanated glass surface and a silanated glass microsphere, immersed in the isotropic phase of the nematic liquid crystal 5CB (4'-*n*-pentyl 4-cyanobiphenyl). At separations of several nanometers, we observed a weak, short range attractive force of the order of 100 pN, which was increased by decreasing the temperature. The temperature dependence of the amplitude and the range of this attractive force can be described by a combination of van der Waals and a mean-field prenematic force due to the surface-induced nematic order. This is supported by ellipsometric study and allows for the determination of the surface coupling energy of 5CB on a silanated glass surface.

DOI: 10.1103/PhysRevE.64.051711

PACS number(s): 61.30.Hn, 68.08.-p, 61.30.Pq, 68.08.Bc

I. INTRODUCTION

Forces between microscopic objects immersed in anisotropic fluids have attracted considerable attention since the recent discovery of nematic emulsions [1–3]. The interest in these composite materials is driven not only by potential optical and electro-optical applications, but also by the scientific aspects of the colloidal interactions in these materials.

The interaction between particles in nematic dispersions is mediated by the elastic distortion of the continuous nematic director field and the van der Waals and electrostatic forces. In this sense, nematic dispersions are anisotropic colloids which are expected to show a variety of interesting anisotropic phenomena. Whereas the nature of director-mediated colloidal interactions has been studied theoretically in several recent publications [1,2,4–9], there is only a very limited number of experimental studies of colloidal forces in anisotropic fluids [10–12]. Moreover, most of these studies have been limited to the temperature range of the nematic phase, whereas the nature of the forces induced by the pretransitional, surface-induced order close to the isotropic phase transition is practically unknown. The experimental observation of these pretransitional, surface-order-induced forces is important, because (i) it gives us direct information on the magnitude and spatial dependence of the surface-induced order, and (ii) it could lead to the observation of the Casimir force in anisotropic fluids [13].

Here we report on measurements of the forces between a micrometer-sized glass sphere and a flat glass surface, separated by a very thin layer of a nematic liquid crystal in the bulk isotropic phase. Both surfaces were coated with a monolayer of *N,N*-dimethyl-*N*-octadecyl-3-aminopropyltrimethoxysilyl chloride (DMOAP) to induce good homeotropic alignment. At separations of the order of the nematic correlation length, we

observe an attractive force between the two surfaces, which is of the order of 100 pN. The magnitude and the range of this attractive force increase as we approach the isotropic-nematic phase transition from above. We explain this temperature dependence by considering a combination of the attractive van der Waals force between the two glass surfaces and the mean-field nematic force, which results from the surface-induced prenematic bridge between the two surfaces. We show that both forces are of comparable magnitude, but can be separated, since the mean-field nematic force is strongly temperature dependent close to the nematic-isotropic phase transition, due to the increasing nematic correlation length and increasing surface order parameter. We support this conclusion by an independent ellipsometric study of the same interface.

II. THEORY

A. Mean-field nematic force

We have used the standard Landau–de Gennes mean-field approach to describe the orientational order of the liquid crystal, where the free energy due to the ordering is expanded in terms of the nematic order parameter. Here, the liquid crystalline order is described by the director field \mathbf{n} and a scalar order parameter S . The director \mathbf{n} is a unit vector pointing in the direction of the average orientation of the molecular long axes of the anisotropic liquid crystalline molecules, and the scalar order parameter S measures how good the alignment of the molecular long axes is with the director. It has been shown by Borštnik and Žumer [9] that the mean-field contribution to the forces between two parallel plates immersed in a partially ordered nematic liquid crystal is always attractive for homeotropic boundary conditions. For curved geometry [14], there is also a small repulsive component due to the distortion of the prenematic director field. This repulsive component is, however, very small compared to the mean-field attractive force and will be neglected in our study.

*Email address: igor.musevic@ijs.si

Following the simplified approach of de Gennes [15], the free-energy density f_B of a bulk nematic liquid crystal can be expanded solely in terms of the scalar order parameter S , if the orientation of the director is homogeneous throughout the sample:

$$f_B = \frac{1}{2} \alpha(T) S^2 + L \left(\frac{dS}{dz} \right)^2. \quad (1)$$

Here, the temperature dependent coefficient $\alpha(T) = a(T - T^*)$ drives the isotropic-nematic transition and L is the elastic coefficient. The nematic correlation length, which measures the length to which the nematic order variation protrudes, is $\xi = \sqrt{L/\alpha}$. We have used the parabolic approximation, which leads to a second order phase transition at T^* . On the other hand, the nematic-isotropic phase transition is weakly first order at T_{NI} , which is typically 1 K above T^* . It can be described by including the third and fourth order terms in the free-energy density expansion. However, as we consider that the nematic order parameter at the surface S_0 is small, the order parameter S is also small and the higher terms in the free-energy expansion [Eq. (1)] can be neglected in the calculation of the order parameter profile at temperatures above T_{NI} .

In the case of a confined liquid crystal, the surface contribution to the total free energy has to be taken into account. The surface energy contribution arises from (i) the breaking of the translation and inversion symmetry due to the presence of the surface and (ii) a direct interaction between the molecules of the surface and the liquid crystal [16,17]. The energy contribution due to the coupling between the homeotropic nematic order and the surface can be expanded as a contact potential in terms of the scalar nematic order on the surface. In the case of a liquid crystal (LC) slab, sandwiched between two planar surfaces located at $\pm d/2$, the surface contribution is

$$f_S = \left(-w_1 S_0 + \frac{1}{2} w_2 S_0^2 \right) \delta(z = \pm d/2). \quad (2)$$

Here, the linear term favors order, whereas the quadratic term favors disorder. Above the nematic-isotropic phase transition temperature T_{NI} , a single flat surface therefore induces a small nematic order S_0 , which decays within a correlation length ξ , as we move from the surface into the isotropic bulk. In the presence of a second flat surface at a distance d , the minimization of the bulk free energy per unit surface area $F_B = \int_{-d/2}^{d/2} f_B dz$, leads, after solving the Euler-Lagrange equations for the free-energy functional f_B , to the order parameter profile $S(z) = S_m \cosh(z/\xi)$, where S_m is the value of the order parameter at the midpoint, i.e., $z=0$. The total free energy per unit surface area of a partially ordered nematic layer, confined between two planparallel plates at separation d , is

$$F(d) = \frac{L S_0^2}{\xi(T)} \tanh\left(\frac{d}{2\xi(T)}\right) - 2w_1 S_0 + w_2 S_0^2. \quad (3)$$

After minimization of $F(d)$ with respect to S_0 , one obtains the equilibrium value of the order parameter at the surface:

$$S_0(d, T) = \frac{w_1}{w_2 + (L/\xi) \tanh(d/2\xi)}. \quad (4)$$

The free energy increases with increasing separation, which means that the prenematic order between two flat confining surfaces induces an attractive mean-field force.

In force experiments, the forces are usually measured between two curved surfaces, such as two crossed cylinders, or between a sphere and a flat surface [18]. In this case, the so-called Derjaguin approximation is used [18], which relates the force between two curved surfaces and the interaction free energy per unit surface area between two flat surfaces. In our case, the force $\mathcal{F}(d)$ between a sphere of radius R and a flat surface is $\mathcal{F}(d) = 2\pi R[F(d) - F(\infty)]$:

$$\mathcal{F}(d) = R w_1^2 \xi(T) \left(\frac{1}{L + w_2 \xi(T)} - \frac{1}{w_2 \xi(T) + L \tanh(d/2\xi)} \right). \quad (5)$$

It is obtained by inserting Eq. (4) into Eq. (3) and subtracting the free energy of the nematic slab between infinitely separated plates. This expression is valid as long as the range of the force, characterized by the nematic correlation length ξ , and the separation d between the two surfaces are small compared to the radius R . The force, which is mediated by the surface-induced nematic order parameter, is attractive and decays approximately exponentially with increasing separation d . The magnitude of the force strongly depends on the surface coupling coefficients w_1 and w_2 . It increases quadratically with increasing w_1 and decreases inversely with w_2 for small separations. The solid line in Fig. 1 shows the calculated separation dependence of the mean-field nematic force between the flat surface and a 5 μ m sphere, using Eq. (5). The Landau-de Gennes material constants for 5CB have been used, $a = 0.13 \times 10^6$ J/m³ K [19] and $L = 6.2$ pN as determined later in the study. To demonstrate the effect of the coupling strength, the force is calculated for two different realistic quadratic surface coupling coefficients $w_2 = 5 \times 10^{-4}$ J/m² and $w_2 = 5.6 \times 10^{-5}$ J/m² at constant linear coupling coefficient $w_1 = 1.2 \times 10^{-4}$ J/m².

For a separation of 4 nm and typical values of the surface coupling coefficients w_1 and w_2 , the amplitude of this force is several 10 pN far beyond the clearing point, and increases to 100–200 pN as we approach the nematic phase from above. In view of the weakness of this mean-field nematic force, which is due to the small value of the surface-induced nematic order S_0 , it is clear that one also has to consider the contributions of other forces, such as the van der Waals force between the sphere and the surface in the presence of a liquid crystal. In Fig. 1, the mean-field nematic force is compared to the van der Waals force between two glass surfaces interacting across an ordered 5CB liquid crystal (dashed line). The Hamaker constant of the van der Waals interaction, $A_{121} = 8.5 \times 10^{-22}$ J, has been calculated according to Eq. (7). It can be seen that the mean-field force is comparable to or weaker than the usual van der Waals force and becomes

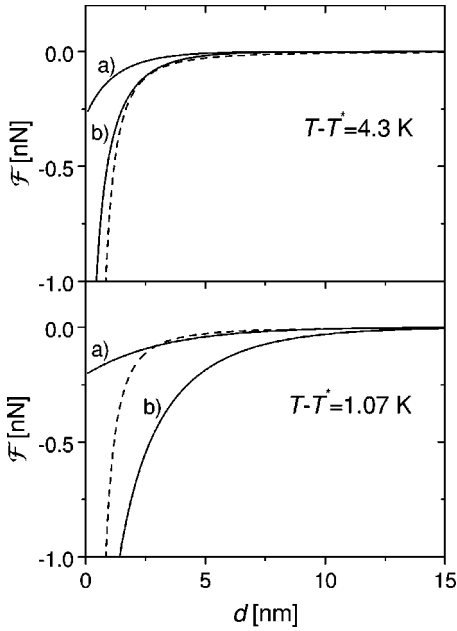


FIG. 1. The separation dependence of the mean-field nematic force between a $5 \mu\text{m}$ sphere and a flat surface inducing homeotropic LC alignment (full lines). The force was calculated from Eq. (5) at two different temperatures above T_{NI} . The force was calculated with two different quadratic surface coupling coefficients w_2 . The curve (a) corresponds to $w_2 = 5 \times 10^{-4} \text{ J/m}^2$ and (b) to $w_2 = 5.6 \times 10^{-5} \text{ J/m}^2$. The linear coupling energy is the same in both cases, $w_1 = 1.2 \times 10^{-4} \text{ J/m}^2$. The Landau–de Gennes parameters for 5CB are used, $a = 0.13 \times 10^6 \text{ J/m}^3 \text{ K}$ [19] and $L = 6.2 \text{ pN}$. The dashed line represents the van der Waals force between the two surfaces, calculated with the Hamaker constant $A_{121} = 8.5 \times 10^{-22} \text{ J}$, which is calculated for the van der Waals interaction between two glass surfaces across the ordered 5CB liquid crystal.

dominant only in the vicinity of the phase transition. Therefore, the van der Waals force has to be considered in the analysis of the detected force, and is discussed in the following section.

B. Van der Waals force in the presence of surface adsorbed layers

In the experimental section it will be shown that the interface between the isotropic phase of a nematic liquid crystal 5CB and a DMOAP coated glass surface has the following structure, as illustrated in Fig. 2. (i) At the DMOAP coated glass surface there is an adsorbed surface layer of 5CB molecules, with a thickness of 3–4 nm. This “first” layer of LC molecules shows nearly smecticlike elastic properties. It is stable even 20 K above the clearing temperature with no detectable changes in thickness and elasticity. (ii) The first molecular layer is followed by a surface-induced paranematic layer that decays within a correlation length away from the surface.

This experimentally observed structure of the interface has important consequences for the van der Waals force between the two glass surfaces. According to the Lifshitz theory of the van der Waals force [18,20], the sign and the magnitude of the Hamaker constant, as well as the separation

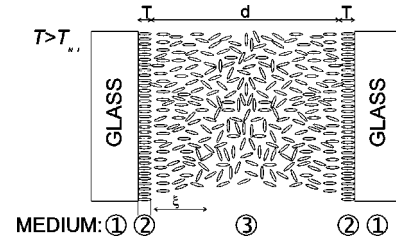


FIG. 2. Structure of the interface of 5CB on DMOAP silanated glass, as deduced from the present atomic force microscopy AFM experiments, performed above the nematic-isotropic phase transition temperature. The first, surface-adsorbed layer of LC molecules shows smecticlike elastic compressibility and is stable more than 20 K above the clearing point. The width of the paranematic layer is of the order of the correlation length ξ and increases as we approach the clearing point from above.

dependence of this force, are strongly influenced by the optical properties and stratification of the medium between the two surfaces. In our case, the following facts have to be considered. (i) The first adsorbed layer of LC molecules is optically uniaxial with the optical axis along the normal to the surface. The Hamaker constant is in this case a complicated function of the ordinary and extraordinary indices of refraction [20]. In our calculation of the Hamaker constant, we neglect dielectric anisotropy and consider an average value of the two refractive indices and dielectric constant for low frequency. (ii) The optical and dielectric properties of the surface-induced paranematic phase are spatially inhomogeneous. To simplify the calculation further, we consider only the spatial average of the index of refraction and dielectric constant in the paranematic phase. As the order parameter profile depends on the separation between the two surfaces, we calculate this average dielectric constant for each separation. The model that follows from these approximations and is a basis for our calculation of the van der Waals force between two surfaces is presented in Figs. 2 and 3. Figure 3(a) shows the order parameter profile across the glass-nematic-glass interface. The order parameter S_0 is constant within the first adsorbed molecular layer of thickness T , and decays continuously to the midpoint value S_m , and again

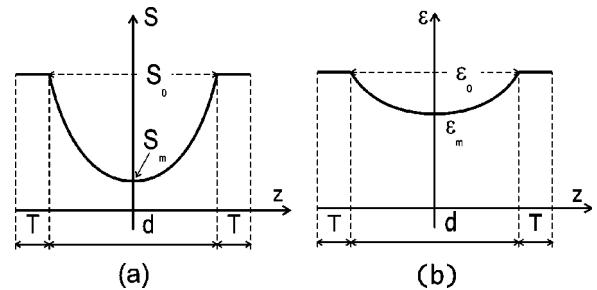


FIG. 3. (a) The order parameter profile used in the analysis of interfacial forces in the isotropic phase of 5CB on a DMOAP silanated glass surface. S_0 is the value of the nematic order parameter at the surface, S_m is the value of the nematic order parameter in the middle of the interface. T is the thickness of the first adsorbed layer of LC molecules and d is the separation. (b) The corresponding profile of the dielectric constant.

increases to S_0 at the neighboring surface. Figure. 3(b) shows the corresponding profile of the dielectric constant: it equals ϵ_0 in the first molecular layer of thickness T and equals ϵ_m in the middle of the surface-induced paranematic layer.

In the Derjaguin approximation, the van der Waals force between a flat glass surface (medium 1) and a sphere of radius R (medium 1), acting across two surface adsorbed layers (medium 2) and a prenematic layer (medium 3) in between, is [18]

$$\mathcal{F}(d)_{vdW} = \frac{R}{6} \left[\frac{A_{232}}{d^2} - \frac{2A_{123}}{(d+T)^2} + \frac{A_{121}}{(d+2T)^2} \right]. \quad (6)$$

Here, A_{232} is the Hamaker constant for the van der Waals interaction between two adsorbed layers (2), across the prenematic layer (3); see Fig. 3. A_{123} is Hamaker constant for the van der Waals interaction between glass (1) and the prenematic layer (3), acting across one adsorbed layer (2). Similarly, A_{121} is the Hamaker constant for the interaction between two glass surfaces (1), acting across two adsorbed layers (2). Using the material parameters for 5CB and BK7 glass, we find that Hamaker constants A_{123} and A_{232} are of the order of $A_{123} \approx A_{232} \approx 10^{-25}$ J. These can be neglected with respect to A_{121} , i.e., the Hamaker constant for the van der Waals interaction between two glass surfaces (1) across a surface adsorbed liquid crystalline layer (2), which is given by

$$A_{121} = \frac{3}{4} k_B T \frac{\left(\epsilon_{glass} - \epsilon_{iso} - \frac{1}{2} X S_0 \right)^2}{\left(\epsilon_{glass} + \epsilon_{iso} + \frac{1}{2} X S_0 \right)^2} + \frac{3}{16\sqrt{2}} h \nu_e \frac{\left[n_{glass}^2 - n_{iso}^2 \left(1 + \frac{1}{12} (\Delta \epsilon_{opt.} / n_{iso}^2) S_0 \right) \right]^2}{\left[n_{glass}^2 + n_{iso}^2 \left(1 + \frac{1}{12} (\Delta \epsilon_{opt.} / n_{iso}^2) S_0 \right) \right]^{21/2}}. \quad (7)$$

Here, ϵ_{glass} and ϵ_{iso} are the static dielectric constants of glass and the isotropic phase of the liquid crystal, respectively. n_{glass} and n_{iso} are the corresponding refractive indices, h is Planck's constant, $\Delta \epsilon_{opt.}$ is the maximum difference in the optical dielectric constants at $S=1$, and ν_e is the electronic absorption frequency of the liquid crystal, which is in the UV range ($\nu_e \approx 3 \times 10^{15}$ s $^{-1}$). The coefficient X describes the increase of the dielectric constant of the liquid crystal due to the enhanced order parameter S_0 and equals $X=6.8$ for 5CB [21]. Similarly, the coefficient $\Delta \epsilon_{opt.}$ describes the increase of the refractive index of the liquid crystal due to the increase of the nematic order parameter S_0 . $\Delta \epsilon_{opt.} = 0.6$ for 5CB [22]. As the surface-induced order parameter in the case of the bulk isotropic phase of a liquid crystal is small, $S_0 \approx 0.1$, the corresponding correction terms in Eq. (7) due to increased nematic order are of the order of only several percent. This means that for most practical pur-

poses, the Hamaker constant for glass-glass interaction across adsorbed liquid crystal layers is essentially temperature independent and is $A_{121} = 8.5 \times 10^{-22}$ J for a glass-5CB-glass system. At a separation of $d=2$ nm and a thickness of adsorbed liquid crystal layers of $T=2.4$ nm, the van der Waals force on a $7 \mu\text{m}$ sphere is attractive and equals 22 pN. It is therefore comparable in magnitude to the attractive mean-field nematic force given in Eq. (5). The main difference is that the van der Waals force is nearly temperature independent, whereas the mean-field nematic force is expected to increase on approaching the nematic-isotropic transition from above.

C. Ellipsometry of the isotropic nematic-glass interface

In an ellipsometric experiment, one measures the state of polarization of light reflected from an interface, which strongly depends on the profile of the dielectric constant across the interface. It is well known that one can determine the values of the surface nematic order parameter S_0 and the nematic correlation length with superior accuracy using Brewster-mode ellipsometry [23]. In this mode of operation, one measures the ellipticity coefficient $\rho = R_p/R_s$ in the vicinity of the Brewster angle, where R_p and R_s are the reflectivity coefficients for p and s polarized light, respectively. For a perfectly sharp and isotropic interface, the ellipticity coefficient equals zero at the Brewster angle, $\rho=0$. However, if the interface is not sharp, but is characterized by the profile $\epsilon(z)$ of the dielectric constant of a given medium, the ellipticity coefficient is finite at the Brewster angle. For the case of an anisotropic and uniaxial medium (such as a liquid crystal) on an isotropic substrate (such as glass), the ellipticity coefficient at the Brewster angle can be expressed in the Drude approximation [24]:

$$\rho = \frac{\pi}{\lambda} \frac{\sqrt{n_{glass}^2 + n_{iso}^2}}{n_{glass}^2 - n_{iso}^2} \times \int_{-\infty}^{\infty} dz \left[n_{glass}^2 + n_{iso}^2 - \frac{n_{glass}^2 n_{iso}^2}{\epsilon_{\parallel}(z)} - \epsilon_{\perp}(z) \right]. \quad (8)$$

Here, λ is the vacuum wavelength of the reflected light, n_{iso} is the index of refraction of the liquid crystal in the isotropic phase, n_{glass} is the refractive index of confining substrate, $\epsilon_{\parallel}(z)$ is the component of the dielectric tensor of the liquid crystal along the normal to the interface, and $\epsilon_{\perp}(z)$ is the corresponding component in the transverse direction. The components of the dielectric tensor depend linearly on the order parameter [10]. This can be written as

$$\begin{aligned} \epsilon_{\perp}(z) &= n_{iso}^2 + \frac{1}{3} \Delta \epsilon_{opt.} S(z), \\ \epsilon_{\parallel}(z) &= n_{iso}^2 - \frac{2}{3} \Delta \epsilon_{opt.} S(z), \end{aligned} \quad (9)$$

where $\Delta \epsilon_{opt.}$ is the maximum anisotropy of the optical dielectric constant at a saturated nematic order parameter $S=1$. In the case of 5CB $\Delta \epsilon_{opt.} \approx 0.6$.

By considering the simple spatial dependence of the order parameter, i.e., $S(z) = S_0 \exp(-z/\xi)$, which solves the Euler-Lagrange equations following from Eq. (1) in the case of a semi-infinite liquid crystal sample, the integral in Eq. (8) can be calculated and the ellipticity coefficient for a partially ordered interface between the isotropic liquid crystal and an isotropic substrate is

$$\rho = \frac{\pi}{\lambda} \frac{\sqrt{n_{glass}^2 + n_{iso}^2}}{n_{glass}^2 - n_{iso}^2} \xi \left[n_{glass}^2 \ln \left(1 - \frac{2\Delta\epsilon S_0}{3n_{iso}^2} \right) - \frac{1}{3} \Delta\epsilon S_0 \right]. \quad (10)$$

In general, the ellipticity coefficient is temperature dependent because of the temperature dependence of the correlation length ξ and S_0 . It increases on approaching the isotropic-nematic phase transition from above. By measuring $\rho(T)$ one can determine the product ξS_0 , and, if we assume a power law dependence of $\xi = \xi(T)$, the temperature dependence of the nematic order parameter at the surface $S_0(T)$ can be extracted.

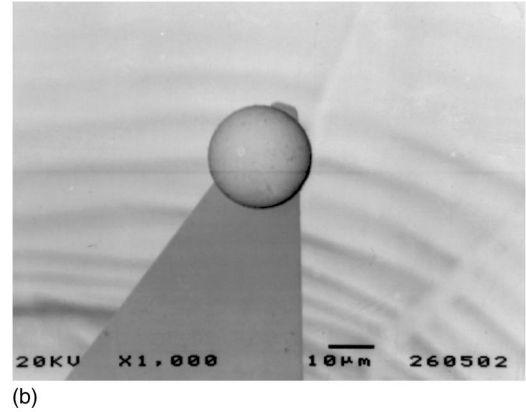
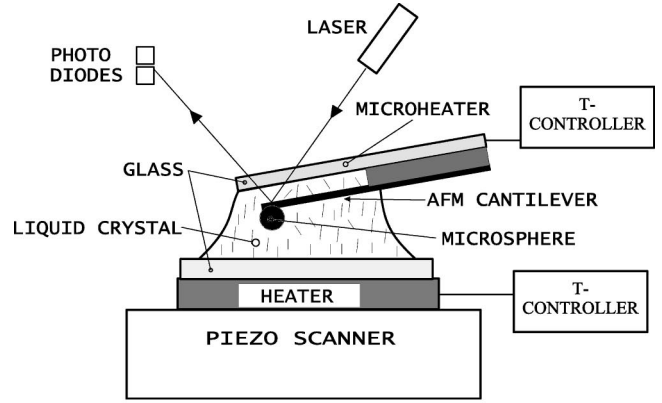
In order to obtain the values of the surface coupling energies from the temperature dependence of S_0 , we have to calculate the value of S_0 for a semi-infinite sample, where the interface is located in the xy plane at $z=0$. The total free energy per unit surface area is $F = F_B + F_S$, where $F_B = \int_0^\infty f_B(z) dz$ and $F_S = w_1 S_0 + \frac{1}{2} w_2 S_0^2$. After minimization with respect to S_0 , the surface value of the order parameter is

$$S_0 = \frac{w_1}{L/\xi + w_2}. \quad (11)$$

III. EXPERIMENT

In our measurements we used a doubly temperature controlled atomic force microscope [25], shown schematically in Fig. 4. (a). The temperature of a liquid crystal is controlled within 5 mK by a small heater, attached directly to the piezo scanner of the AFM. A second microheater is attached above the AFM cantilever in order to reduce the temperature gradients in the liquid crystal, which fills the space between the lower glass plate and the upper heater. In this geometry, the AFM cantilever and the AFM probe are completely immersed in liquid crystal and there are no stray capillary forces, except for the interfacial force between the AFM probe and the surface of the glass.

In order to expand the accessible range of forces exerted on the surface, we used two different AFM probes in our experiments. In the first set of experiments, cantilevers with sharp Si_3N_4 tips (Park Scientific) were used. The force constants of the cantilevers ranged from 0.01 N/m to 0.1 N/m and the radius of the tip was typically 20 nm. Force constants were taken as reported by the manufacturer. Using these sharp cantilevers, relatively large force loads can be applied to the interfacial structure and one can eventually detect (and image) the first surface adsorbed layers of molecules. In the second set of experiments, an $R=7 \mu\text{m}$ glass sphere was attached to the cantilever [see Fig. 4(b)] and the force between the sphere and the flat surface was measured in the presence of the isotropic nematic phase.



(a)

(b)

FIG. 4. (a) The setup of the temperature controlled AFM. Two independent microheaters are used to control the temperature of a liquid crystal with an accuracy better than 5 mK in the temperature range up to 350 K. For details, see Ref. [25]. (b) Glass microsphere, attached to the AFM cantilever, is used in the measurements of paranematic interfacial forces.

The glass substrates and glass spheres were carefully cleaned in detergent, rinsed in pure water, and finally rinsed with acetone. After that, a monolayer of DMOAP was deposited on the glass surface from a water-methanol solution. We used a 1% water solution of 50% DMOAP-methanol solution (ABCR, Germany). Twice distilled water was used. The glass plate was left in the freshly prepared solution for 5 min and carefully rinsed with distilled water and isopropanol after that. The glass surface was rendered highly hydrophobic and the alignment of 5CB nematic liquid crystals on these surfaces was perfectly homeotropic and stable, as checked with a polarizing microscope on extra samples. The AFM sharp probes were used with no modifications and cleaning, but a new probe was used in each experiment.

The experiments were performed in several experimental runs at room condition. In each run, the AFM was thermalized for one day, with the microheater turned on. After that, a liquid crystal in its isotropic phase was introduced between the glass substrate and the AFM probe, and again thermalized for several hours. The experiment was then performed in a single experimental run that typically lasted for 6–8 h. At each temperature, a large number of force-versus-distance plots were recorded and the results of the fits were averaged for each temperature. We have observed a significant aging

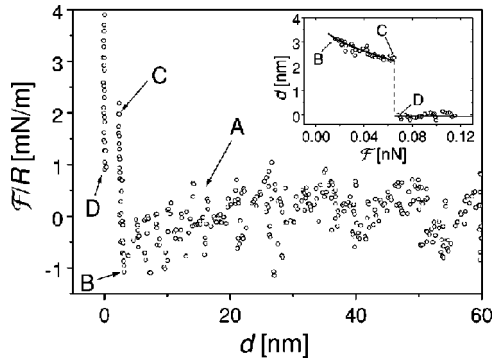


FIG. 5. Compression and rupturing of the first, surface adsorbed layer of 5CB molecules on silanated glass. The force on the AFM tip is shown as a function of separation d at a temperature 2 K above the bulk clearing point. The solid line in the inset is the best fit to the Hertz theory of indentation with compressibility modulus $E=(7.8 \times 10^6)(1 \pm 0.4)$ N/m².

of the DMOAP–liquid-crystal interface during the first 24 h. The roughness of the interface, as measured by AFM, increased significantly during this time period. This indicates a process of adsorption of impurities from the liquid crystal onto the DMOAP surface, to our knowledge not reported before by others. All the results reported in this paper were collected within the first 24 h after starting the experiment.

The AFM was used in the so-called force plot mode of operation, where the piezo scanner of the AFM and the substrate perform time-periodic linear movements in the direction of the AFM tip. The speed of approach is several nm/s and at the same time the deflection of the AFM cantilever is monitored. In this way, one obtains the force-versus-separation plots. The zero of the separation was determined from the point of a hard contact between the sharp AFM probe and the substrate.

The ellipsometric experiment in the Brewster mode was performed using a phase-modulated ellipsometer [23]. The ellipsometer was continuously scanning in the vicinity of the Brewster angle [26], whereas the temperature was varied continuously at a rate of several K/h.

IV. RESULTS AND ANALYSIS

In the first set of experiments, we used sharp tips with a typical radius of curvature of $R=20$ nm, to probe the forces at the interface of isotropic 5CB and silanated glass. A typical force plot is shown in Fig. 5.

At large separations d , there is essentially no force on the AFM tip. However, at a separation of several molecular lengths, the tip is attracted toward the surface (point A to point B). The attractive force is of the order of 10^{-11} N and the tip comes to force equilibrium at a distance of 1–2 molecular lengths away from the surface. After that, the cantilever starts to compress the material between the tip and the surface, until it reaches point C, indicated in Fig. 5. Here, the tip suddenly penetrates the surface adsorbed molecular layer and comes into close contact with the surface, indicated by D. This happens at a tip-surface separation of typically

2 nm, which is close to the length of a single liquid crystalline molecule.

Let us first consider the compression of the surface adsorbed molecular layer from point B to the point of rupturing. For small force loads, the thickness of this layer is ≈ 3 nm. By increasing the force of the AFM tip, the layer compresses to ≈ 2 nm and then ruptures at a force load of ≈ 60 pN. By performing trace-retrace experiments, we have observed that the compression of this layer is purely elastic, with no hysteresis indicating plastic deformation. We have also made sure that this layer cannot be attributed only to the silane monolayer by performing the same force experiment using hexane instead of the liquid crystal, where no rupturing could be observed. We have followed the temperature stability of the first molecular layer deep into the isotropic phase, as it can be observed more than 20 K above T_{NI} . In this temperature range the layer shows no change of compressibility modulus or thickness, which is a clear indication of a very strong coupling of the first layer of liquid crystalline molecules to the substrate.

The compression of the first layer of liquid crystal molecules was analyzed using Hertz theory for the indentation of a flat surface of a softer material by the rigid spherical AFM tip of radius R [27]. The depth of indentation is $\delta = \sqrt[3]{(9\mathcal{F}^2)/(16RE^{*2})}$, where \mathcal{F} is the force applied to the spherical tip and $E^*=E/(1-\nu^2)$, where E is the Young's elastic modulus of the surface layer and ν is the corresponding Poisson's number. The solid line in the inset to Fig. 5 shows the fit to the Hertz theory. The elastic modulus of the first molecular layer of 5CB is $E=(1 \times 10^7)(1 \pm 0.15)$ N/m², which is typical for a smectic liquid crystal [28]. This suggests that the first, surface adsorbed layer of liquid crystalline molecules is smecticlike at temperatures where the bulk liquid crystal is in the isotropic phase.

The pre-nematic forces on the sharp, nanometer-sized AFM tip are too small to be detected by the AFM. We therefore measured the separation dependence of the interfacial forces using a silanated glass sphere of $R=7$ μ m, attached to the AFM cantilever. The results for 5CB are shown in Fig. 6 for two different temperatures above T_{NI} .

In all cases one can clearly see an attractive, short range force, acting on the sphere. At higher temperatures, the range and the amplitude of this force are small, whereas close to T_{NI} the range and magnitude of the force obviously increase.

We have fitted this attractive force using the sum of the nematic mean-field force given in Eq. (5) and the van der Waals force $F(d)_{vdW}=A_{121}R/[6(d+2T)^2]$ as discussed in Sec. II B. The Hamaker constant A_{121} and the thickness of the adsorbed smecticlike layer T have been taken to be constant with values 8.5×10^{-22} J and 2.8 nm, respectively. The thickness of the surface adsorbed layer was determined in experiments with a sharp AFM tip as described before. From the fits shown in Fig. 6, one can see good agreement between the theory and experiment.

In addition, ellipsometry measurements of the temperature dependence of the ellipsometric ratio at the Brewster angle have been performed and compared to the results of the force spectroscopy. The ellipticity coefficient for 5CB on

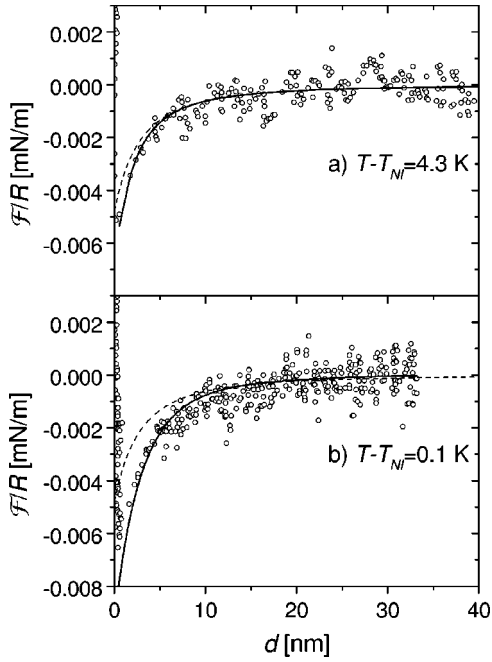


FIG. 6. The attractive force on a $7 \mu\text{m}$ glass microsphere, as a function of separation d from the second glass surface, measured in the presence of 5CB at two different temperatures in the isotropic phase. Both surfaces are covered with a monolayer of DMOAP. The solid lines are the best fits to the sum of mean-field nematic and van der Waals forces, as described in Secs. IV and II. The dashed line shows the contribution of the van der Waals force.

a DMOAP silanated BK7 glass substrate is shown in Fig. 7.

The temperature dependence of the ellipticity coefficient was fitted to Eq. (10), taking the value of the nematic order parameter on the surface S_0 given by Eq. (11). Several parameters have to be varied in the fitting procedure. We wanted to determine both coupling energies w_1 and w_2 , but at the same time we had to allow variation of the supercooling temperature limit T^* , elastic constant of the free energy expansion L , and nematic correlation length $\xi(T)$. The following constraints were used in the fitting procedure: (1) When only the quadratic terms in the free-energy expansion are considered, the nematic correlation length is $\xi(T) = \xi_0 / \sqrt{T - T^*}$, where $\xi_0 = \sqrt{L/a}$. a has been taken as an

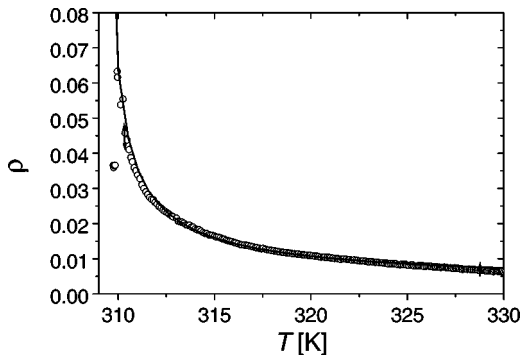


FIG. 7. The temperature dependence of the ellipticity coefficient for 5CB on a DMOAP silanated BK7 glass surface. The solid line is the best fit to Eqs. (10) and (11).

independent parameter, given by Coles [19] and also independently verified in our dynamic light scattering experiments. (2) The difference between the phase transition temperature and the supercooling limit T^* is in the range $0.8 \text{ K} < (T_{NI} - T^*) < 1.6 \text{ K}$. In our analysis we have therefore determined the coupling energies w_1 and w_2 , bare correlation length ξ_0 , and supercooling limit temperature.

In order to obtain the most probable values of these parameters, we have iteratively fitted the ellipsometric and AFM force measurements to the models described before. We have also taken advantage of the fact that the parameters are encountered differently in the expressions for the ellipticity coefficient and the mean-field nematic force. Since both coupling constants depend critically on each other in the ellipsometry, we fixed one of them in the fitting procedure. For example, we performed several fits with different values of fixed w_2 and found the best agreement for $w_2 = (7 \times 10^{-4})(1 \pm 0.4) \text{ J/m}^2$ and $w_1 = (1.6 \times 10^{-4})(1 \pm 0.1) \text{ J/m}^2$. At the same time we iteratively fitted several force measurements at different temperatures and took into account the values obtained from analysis of the ellipsometric measurements. In this way we determined the surface coupling constants $w_1 = (1.4 \times 10^{-4})(1 \pm 0.4) \text{ J/m}^2$ and $w_2 = (7 \times 10^{-4})(1 \pm 0.3) \text{ J/m}^2$. From the force measurements we were able to directly determine the temperature dependence of the nematic correlation length. Then the bare correlation length ξ_0 was iteratively varied to give the best agreement between the sets of coefficients determined in the ellipsometry and in the force measurements. The bare correlation length was finally set to $6.2 \text{ nm K}^{0.5}$, which is in good agreement with the results of other authors. From the bare correlation length, the elastic coefficient was estimated to be $L = 6.2 \text{ pN}$. The solid lines in Figs. 6 and 7 are plotted with this set of parameters, $w_1 = 1.5 \times 10^{-4} \text{ J/m}^2$, $w_2 = 7 \times 10^{-4} \text{ J/m}^2$, and L as given above, and one can see reasonable agreement.

V. CONCLUSIONS

In conclusion, we have observed a temperature dependent mean-field prenematic force between silanated glass surfaces, using force spectroscopy. The observed magnitude of the force, as well as its temperature dependence, are in good agreement with the predictions of the Landau-de Gennes theory. The magnitude of the surface-induced mean-field nematic force depends critically on the surface preparation. In other measurements on the same system, where the glass surface was additionally cleaned in oxygen plasma prior to the deposition of DMOAP, a capillary condensation of nematic liquid crystal between glass surface and sphere was observed as reported elsewhere [29]. In that case the surface preferred order was much stronger.

The results of the AFM force measurements were compared to the results of Brewster angle ellipsometry on similar surfaces. We found reasonably good agreement of the two experiments and were able to determine the surface coupling parameters and elastic constant of the nematic order for a 5CB nematic liquid crystal on DMOAP covered surfaces.

Finally, we would like to comment on the observability of

the Casimir fluctuation force near the isotropic-nematic phase transition. The idea behind force experiments in liquid crystals is that the Casimir force could be separated from other relevant forces in this system, as the range of the Casimir force increases due to increasing correlation length, when approaching the phase transition from above. However, it is clear from our experiment that the Casimir fluctuation

force is very difficult to separate from the mean-field nematic force, which is quite strong and even dominating in the vicinity of the clearing point. It is also clear that the only possibility for observing the Casimir force is the case when the mean-field nematic force is suppressed by suitable boundary conditions [30]. This, however, remains open for future force experiments.

-
- [1] P. Poulin, H. Stark, T.C. Lubensky, and D.A. Weitz, *Science* **275**, 1770 (1997).
- [2] P. Poulin and D.A. Weitz, *Phys. Rev. E* **57**, 626 (1998).
- [3] J. Jamamoto and H. Tanaka, *Nature (London)* **409**, 321 (2001).
- [4] T.C. Lubensky, D. Petey, N. Currier, and H. Stark, *Phys. Rev. E* **57**, 610 (1998).
- [5] A. Poniewierski and T.J. Sluckin, *Liq. Cryst.* **2**, 281 (1987).
- [6] S. Ramaswamy, R. Nityananda, V.A. Raghunathan, and J. Prost, *Mol. Cryst. Liq. Cryst. Sci. Technol., Sect. A* **288**, 175 (1996).
- [7] O.V. Kuksenok, R.W. Ruhwandl, S.V. Shiyonovskii, and E.M. Terentjev, *Phys. Rev. E* **54**, 5198 (1996).
- [8] R.W. Ruhwandl and E.M. Terentjev, *Phys. Rev. E* **55**, 2958 (1997).
- [9] A. Borštnik and S. Žumer, *Phys. Rev. E* **56**, 3021 (1997).
- [10] R.G. Horn, J.N. Israelachvili, and E. Perez, *J. Phys. (France)* **42**, 39 (1981).
- [11] P. Poulin, V. Cabuil, and D.A. Weitz, *Phys. Rev. Lett.* **79**, 4862 (1997).
- [12] M. Ruths, S. Steinberg, and J.N. Israelachvili, *Langmuir* **12**, 6637 (1996).
- [13] A. Ajdari, L. Peliti, and J. Prost, *Phys. Rev. Lett.* **66**, 1481 (1991).
- [14] A. Borštnik, H. Stark, and S. Žumer, *Phys. Rev. E* **60**, 4210 (1999).
- [15] P.G. de Gennes, *Langmuir* **6**, 1448 (1990).
- [16] M.A. Osipov, T.J. Sluckin, and S.J. Cox, *Phys. Rev. E* **55**, 464 (1997).
- [17] A.K. Sen and D.E. Sullivan, *Phys. Rev. A* **35**, 1391 (1987).
- [18] J. Israelachvili, *Intermolecular and Surface Forces* (Academic Press, San Diego, CA, 1992).
- [19] H.J. Coles, *Mol. Cryst. Liq. Cryst.* **49**, 67 (1978).
- [20] J. Mahantya and B.W. Ninham, *Dispersion Forces* (Academic Press, San Diego, CA, 1976).
- [21] A. Buka and L. Bata, *Mol. Cryst. Liq. Cryst.* **49**, 135 (1986).
- [22] R. Horn, *J. Phys. (France)* **39**, 105 (1978).
- [23] D. Beaglehole, *Mol. Cryst. Liq. Cryst.* **89**, 319 (1982).
- [24] J. Lekner, *Theory of Reflection* (Martinus Nijhoff Publishers, Boston, 1987).
- [25] I. Muševič, G. Slak, and R. Blinc, *Rev. Sci. Instrum.* **67**, 2554 (1996).
- [26] R. Lucht, C. Bahr, G. Heppke, and J.W. Goodby, *J. Chem. Phys.* **108**, 3716 (1998).
- [27] K.L. Johnson, *Contact Mechanics* (Cambridge University Press, Cambridge, UK, 1985).
- [28] J. Yamamoto and K. Okano, *Jpn. J. Appl. Phys., Part 1* **30**, 754 (1991).
- [29] K. Kočevár, A. Borštnik, I. Muševič, and S. Žumer, *Phys. Rev. Lett.* **86**, 5914 (2001).
- [30] P. Zihlerl, R. Podgornik, and S. Žumer, *Chem. Phys. Lett.* **295**, 99 (1998).